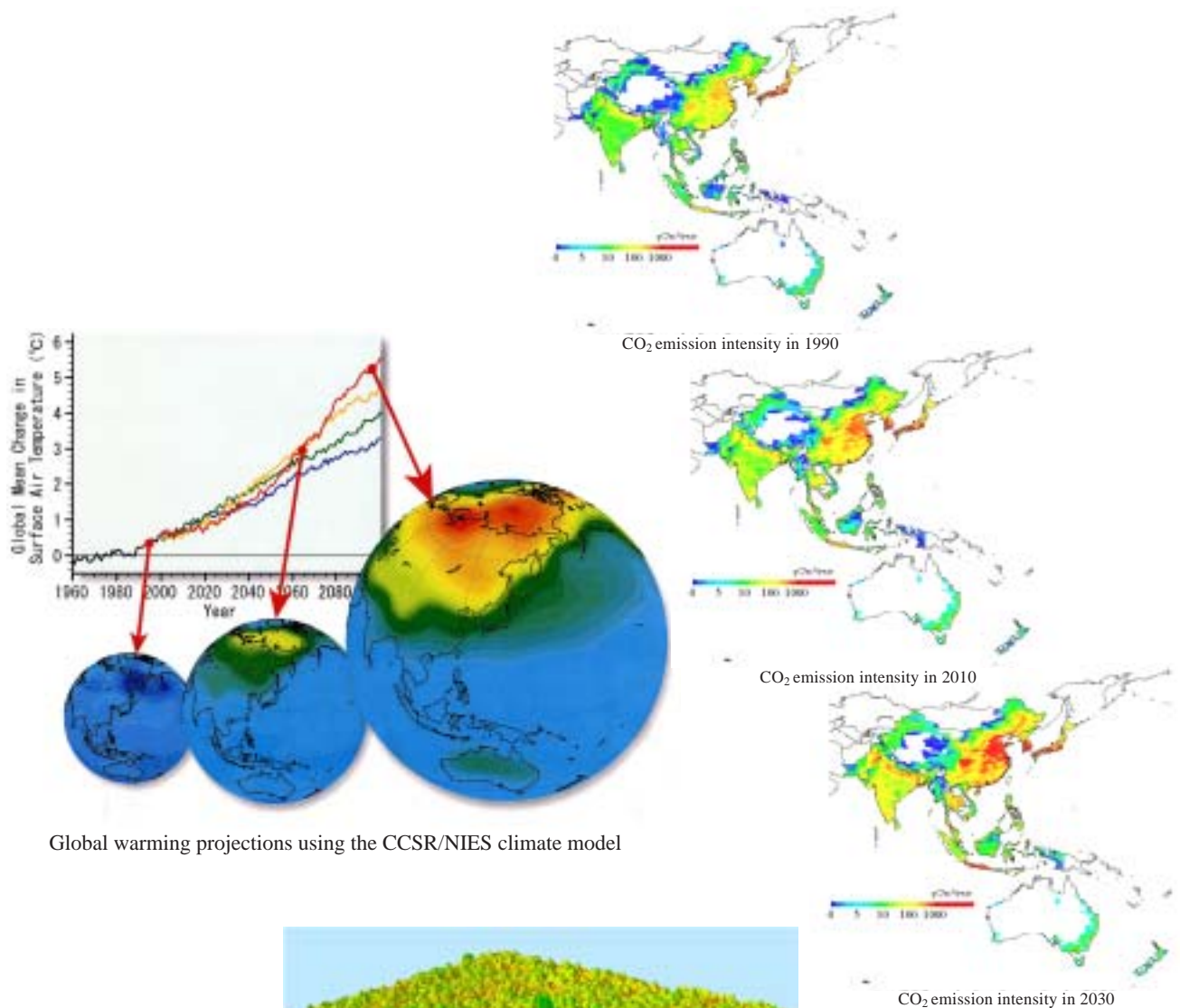
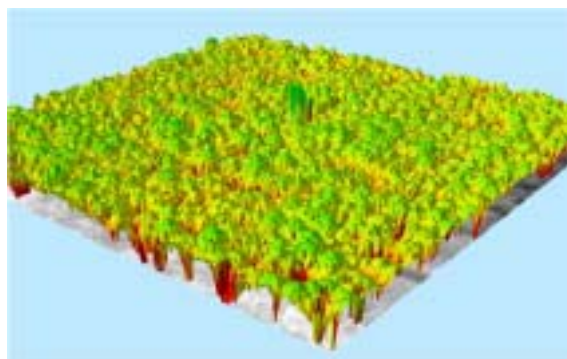


# Climate Change Research Project



Global warming projections using the CCSR/NIES climate model



3D View of Canopy Digital Surface Model using airborne laser data.

### Sub-project on carbon cycle research

This sub-project was initiated to determine the patterns and driving forces of the carbon cycle among anthropogenic sources and the pools of atmospheric, biospheric, and oceanic carbon. The two research teams involved in this sub-project are the **Carbon Cycle Research Team** and the **Carbon Sink Assessment Team**. This year we are reporting on the atmospheric research activities of the Carbon Cycle team; the activities of the Carbon Sink team will be discussed in later reports.

#### 1. Analysis of carbon sink ratio between land and ocean from changes in the atmospheric oxygen concentration and stable carbon isotope ratio.

Increases in the carbon dioxide concentration in the atmosphere as a result of anthropogenic activities will lead to climate change on a global scale. About 60% of the total anthropogenic emission accumulates in the atmosphere, and the sinks in the terrestrial ecosystem and the ocean are remarkable. The partitioning between terrestrial and oceanic sinks changes from year to year, and the driving force behind this change is an urgent research target, because it will be the key to predicting future atmospheric CO<sub>2</sub> concentrations under climatic change.

The atmospheric oxygen concentration is decreased by fossil fuel burning and increased by photosynthesis. The oxygen concentration by solution of CO<sub>2</sub> into ocean does not change. In this project, we are monitoring the oxygen concentration in the atmosphere at Hateruma and Ochi-ishi ground-base monitoring stations (Y. Tohjima) (Fig. 1).

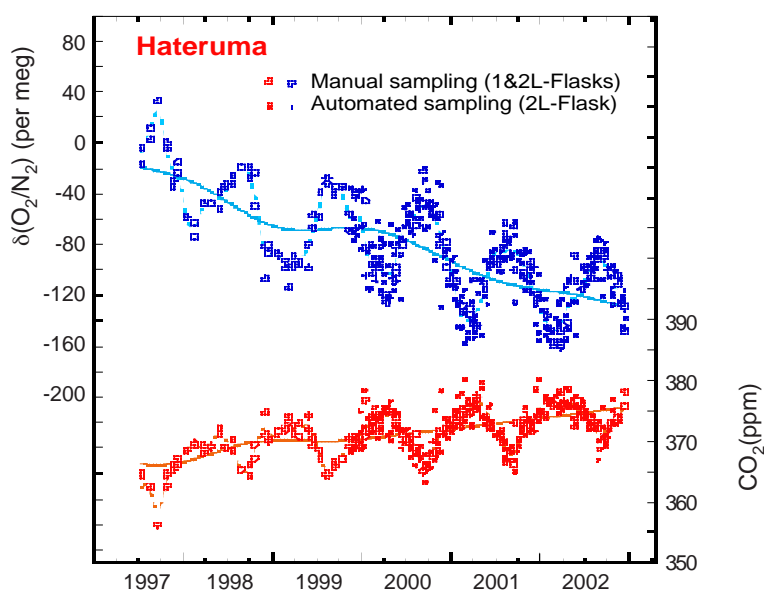


**Fig. 1**  
Six-year record of O<sub>2</sub>/N<sub>2</sub> ratio and CO<sub>2</sub> concentration observed at Hateruma Station.

This monitoring began in 1997 with monthly sampling followed by laboratory analysis by gas chromatography–thermal conductivity detection. The sampling frequency was increased to every fourth day in 1999. From the annual change of  $-19.1 \pm 1.0$  per meg/y and  $1.61 \pm 0.15$  ppm/y for O<sub>2</sub> to N<sub>2</sub> ratio and CO<sub>2</sub> concentration, respectively, and the input to the atmosphere of CO<sub>2</sub> from fossil fuel as 0.2 Gt C/y, we calculated

the terrestrial sink to be  $0.7 \pm 0.4$  Gt C/y and the oceanic sink to be  $2.5 \pm 0.7$  Gt C/y. These values are tentative because they cover only a limited period of observation; further research is required to give more reliable values.

In a similar manner, the stable carbon isotope ratio in atmospheric carbon dioxide is influenced by fossil fuel combustion and the sink ratio between the land and ocean. There is a trend of decrease in the heavy isotope ratio because fossil fuel origin is light-carbon rich. Analysis of isotope ratios in air sampled from ships of opportunity sailing between Japan and Australia has been conducted since 1995 (H. Mukai). From the average isotope ratios in latitudes ranging from S25° to N50°, we evaluated the carbon sinks in the terrestrial ecosystem and the ocean, and plotted them in Fig. 2, together with anthropogenic CO<sub>2</sub> input, southern oscillation index (SOI) and temperature anomalies of the southern hemisphere. There was a good correlation between high temperature and small land sink or land source (Fig. 2).

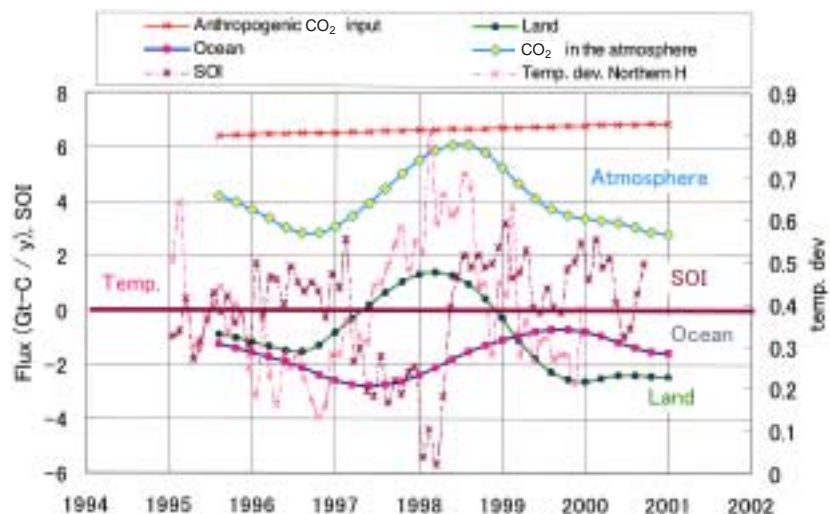


**Fig. 2**  
Change of ocean and land sink strengths in the latitude range S25°–N50°, and controlling parameters.

### Estimation of sink distribution in continents by atmospheric CO<sub>2</sub> distribution measurements: a top-down approach to carbon sinks

One promising approach to the identification of the sink–source distribution of carbon over continents is the estimation from atmospheric carbon dioxide distribution.

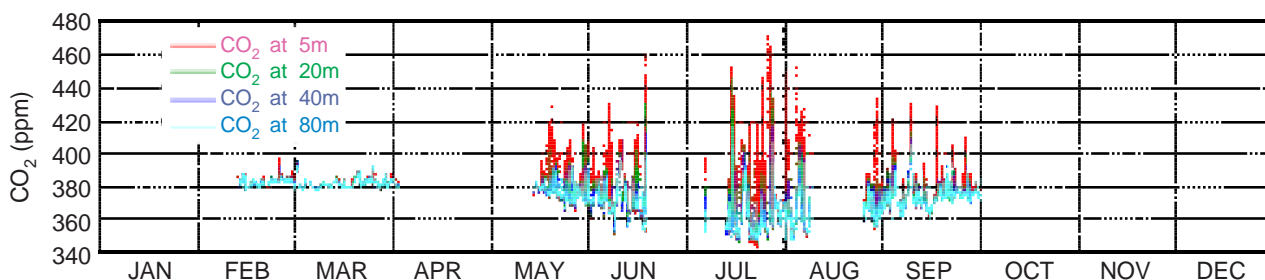
A sink–source interface exists on the surface, and air that has interacted with the surface is transported elsewhere, resulting in a three-dimensional carbon dioxide distribution. This process can be simulated by using a sink–source model and an atmospheric transport model, then, the agreement between simulated and observed distributions can be maximized by adjusting the sink–source pattern within various boundaries. This process is called as Inverse Model Analysis. This approach has been successful in identifying sink–source distribution on a sub-continental scale; by dividing the Earth’s surface into 22 areas.

Our research aim was to apply this method on a smaller scale to obtain a much more precise sink–source distribution, and to compare the results with those of a carbon

budget model that combines ground-based flux measurement and a scaling-up process that uses satellite data. One key to the scaled-down inverse model analysis is a better understanding of CO<sub>2</sub> transport within the boundary layer and the interaction between the boundary layer and the free troposphere.

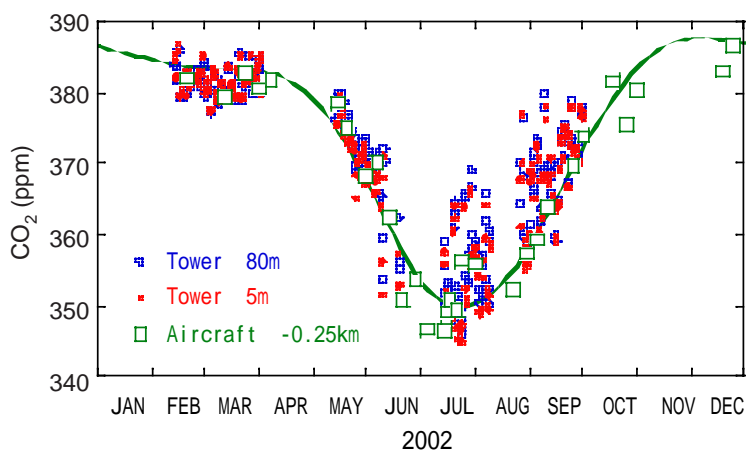
A pilot study of the network was started in 2001, and the first full year's data were obtained in 2002 (Machida and Watai). The monitoring site is at Beresorechika village, lat 56°10'N, long 84°20'E, northwest of Tomsk, in West Siberia. The air is sampled from a telecommunications tower and analyzed by a system developed in 2001. The CO<sub>2</sub> concentration 80m from the ground is constant in winter. It begins to decrease in mid-May, when forest photosynthesis becomes active, and is at a minimum at the end of July (Fig. 3). The concentration at 5 m shows similar behavior, but the night-time concentration in summer is more than 100 ppm higher than the daytime value.

**Fig. 3**  
Seasonal variation in atmospheric CO<sub>2</sub> observed at Beresorechika Village in West Siberia.



We also performed observations from aircraft over the tower and obtained seasonal values at different heights from 100 to 3000 m (Fig. 4). When the lowest-level data obtained by aircraft were compared with ground-based daytime data, the aircraft values fitted the minimum envelope curve of the ground data (Fig. 4), because the aircraft observations were performed under a clear sky at midday. This result suggests that the ground-based data represent the mixing layer concentration of CO<sub>2</sub> when convective mixing is strong.

**Fig. 4**  
Seasonal fluctuation in daytime atmospheric CO<sub>2</sub> concentration at 250 m height, obtained by aircraft observation (green squares), and at 80 m (blue circles) and 5 m (red dots).



### Sub-project on climate change scenarios and comprehensive mitigation strategies based on integrated assessment models

This sub-project resulted from the outcomes of research over the past 10 years at NIES and aims to address new policy needs arising from the Kyoto Protocol, post-Kyoto negotiations, and long-term integration between climate and sustainable development policies. The target of this sub-project is to develop a set of models for integrated assessment of economic growth, climate change, and their impacts. These models will then be used to help estimate the effects of Kyoto and post-Kyoto interventions on global climate change and its regional impacts. The sub-project is also expected to identify the most effective future strategies for integrating sustainable development in Asia and climate change mitigation under alternative paths of future development.

The 3 research teams involved in this sub-project—the Socioeconomic and Emission Modeling Team, the Climate Model Research Team, and the Impact and Adaptation Modeling Team—achieved the following outcomes in FY 2002.

The **Socioeconomic and Emission Modeling Team** used an emission model for greenhouse gases (GHGs) and air pollutants for scenario analyses of major Asian countries (Japan, China, India, Korea, Thailand, Malaysia, Vietnam). The model simulates choices of technologies for producing goods and services that enable the user to assess the cost of GHG mitigation, the effect of economic interventions such as carbon taxes, and the achievable levels of energy and emission intensity (Fig. 5). The Emission Modeling Team also refined the economic model to consider energy and material flow in an integrated way. This model was used to investigate environmental degradation (including the effect of recycling policies) in India and China. The team is now developing a new multi-regional general equilibrium model. A detailed database for the energy sector, an important component of this model, was developed this year.

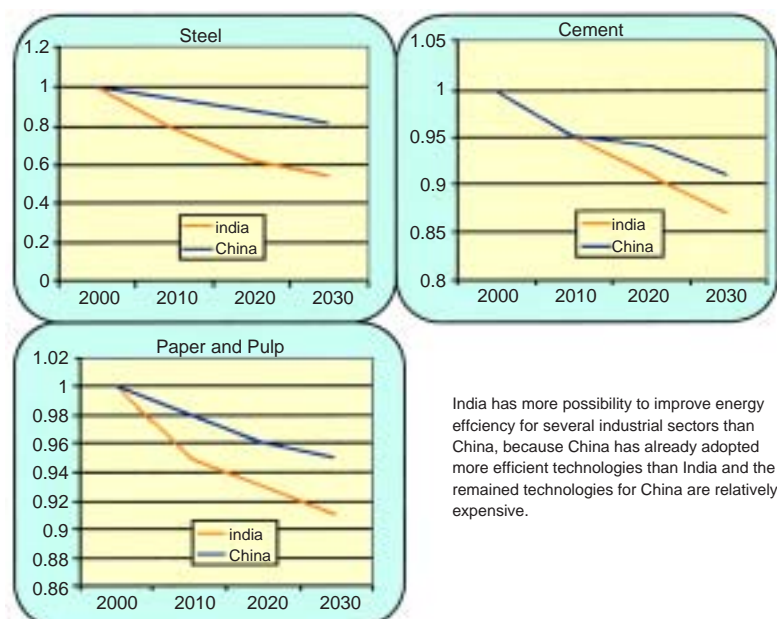


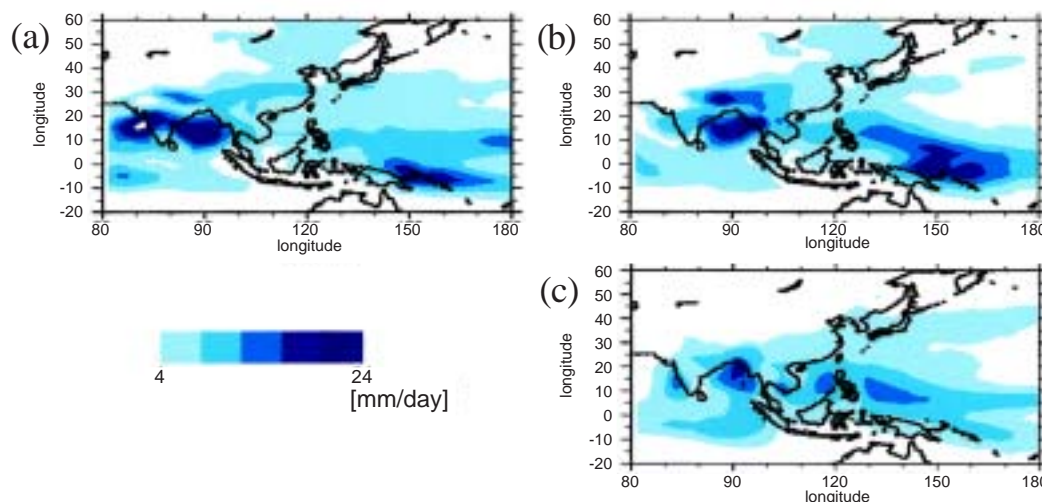
**Fig. 5**  
Projected energy intensities of the steel, cement and paper, and pulp industries in China and India from 2000 to 2030, simulated by AIM.

India has more possibility to improve energy efficiency for several industrial sectors than China, because China has already adopted more efficient technologies than India and the remained technologies for China are relatively expensive.

The **Climate Model Research Team** improved the performance of their global climate model by revising the simulated processes. This revised formulation, along with a new input for cumulus convection, improved the representation of summer precipitation in Asia (Fig. 6). Further, refinement of the land surface model and the introduction of direct and indirect aerosol effects improved the representation of vapor pressure in the air close to the land surface in continents of the northern hemisphere. The Climate Model Team is also developing an interface to facilitate linkage between the emission model study and the climate model study. In this regard, a tool for producing grid data on aerosol emissions with a spatial resolution of  $0.5^\circ \times 0.5^\circ$  from country-wide aerosol emission statistics was developed this year.

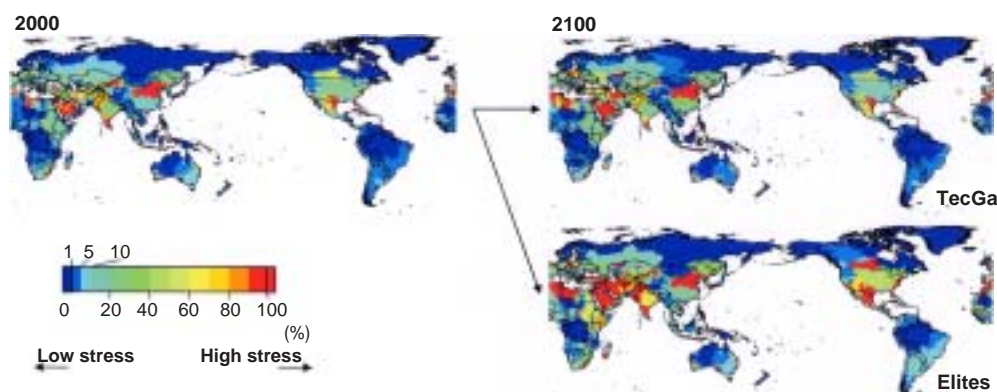
**Fig. 6**  
Summer precipitation in Asia.

- (a) Result of simulation performed with the old version of the models.
- (b) Results of simulation performed with the new version of the model, with the revisions mentioned in the text.
- (c) Spatially interpolated data derived from climatological observations.



The **Impact and Adaptation Modeling Team** developed a distribution package for impact models, tools, databases, and visualization modules, with an interface that enables these elements to be used in an integrated way. The package will be publicly distributed through the web site. We expect that the package enable researchers in developing countries to assess national-scale impacts independently. The Impact Team also refined its water resource model and assessed the future water stresses in each global river basin (Fig. 7). The risk of water shortage will increase, especially in developing countries, as a result of population growth and rapid industrialization. Climate change would add to this water stress in regions where precipitation is projected to decrease.

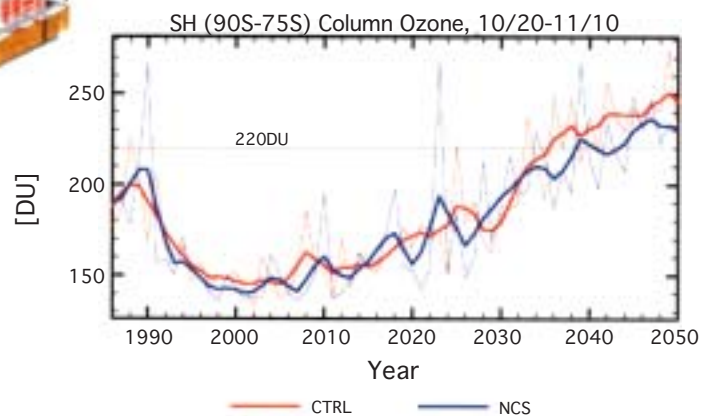
**Fig. 7**  
Current and projected Water Stress Index under different future scenarios of world development. Water Stress Index = water withdrawal / renewable water resource  
TecGa: Future world that assumes globalization, rapid technological improvement, low population increase and high environmental consciousness.  
Elites: Future world that assumes regionalization, slow technological improvement, high population increase and low environmental consciousness.



# Ozone Layer Research Project



Stratospheric ozone layer observation  
by ILAS-II onboard ADEOS-II.



Temporal profiles of column ozone in the ozone hole simulated under the conditions of increasing (CTRL) and fixed (NCS) CO<sub>2</sub>

### **Background and Purpose**

To counter the problem of ozone depletion due to specific chlorofluorocarbons, bromofluorocarbons, and other substances, various measures have been taken by a number of governments in accordance with the Vienna Convention for the Protection of the Ozone Layer, the Montreal Protocol on Substances that Deplete the Ozone Layer, and other relevant international agreements. As a result, the total content of organic halogen compounds that are destroying ozone layer has started to decrease, even in the stratosphere. Nevertheless, the Antarctic ozone hole still appears to be growing larger every year, even considering its great annual variation, and springtime ozone depletion over the Arctic is increasing. Therefore, it may not be appropriate to predict the scale of ozone depletion by chlorine content alone. Continuous monitoring of the stratospheric ozone layer is required to explore how the ozone layer changes with the decreasing halogen concentration in the stratosphere. We also need to accumulate scientific knowledge on the meteorological conditions and climate of the stratosphere, as well as on the physical and chemical processes that affect the depletion of the ozone layer. Together with the Ministry of the Environment (MOE), we have been monitoring the ozone layer by using a satellite-borne ozone sensor and ground-based remote-sensing equipment, analyzing the data obtained, and conducting research using numerical models.

The stratospheric ozone layer over both poles (high latitude regions) is considered to be the most susceptible to changes in various ozone-depleting factors, including the concentrations of halogen species, temperature, and the strength of the polar vortex. The stratospheric ozone layer over the mid-latitudes seems to be susceptible to changes in transport processes and to in situ chemical ozone loss. Accordingly, we have been monitoring, and will continue to monitor, the ozone layer by using satellite-borne sensors for the high-latitude regions and ground-based remote-sensing equipments for the mid-latitudes. We have gathered data both within and outside Japan to help monitor and identify the mechanisms of change in the ozone layer. The project also conducts data analysis and numerical modeling to accumulate scientific knowledge on the mechanisms of change in the ozone layer, thus contributing to the prediction and validation of future ozone layer changes.

### **Objectives**

The 5 main objectives for the mid-term stage of this project are: 1) provision of new versions (5.20 and 6.0) of validated Improved Limb Atmospheric Spectrometer (ILAS) data products to the scientific community; 2) acquisition and processing of ILAS-II data (ILAS-II is a satellite-borne ozone layer monitoring sensor developed by MOE to provide ILAS-II data products both within and outside Japan for scientific use, such as research and monitoring of the ozone layer. It launched on 14 December 2002); 3) continued ground-based ozone layer monitoring at Tsukuba (NIES) and Rikubetsu (Rikubetsu Integrated Stratospheric Observation Center) for registration of the obtained data in the Network for Detection of Stratospheric Change (NDSC) international database, and provision of the data to organizations both within and

outside Japan; 4) identification of the role played in polar ozone layer changes by processes involving physically and chemically important elements, and identification of the mechanisms of these processes; and 5) validation of predicted future ozone layer changes as a basis for formulating measures to protect the ozone layer, and validation of the latest predicted ozone layer changes to provide expert knowledge for evaluating the effectiveness of these protection measures.

### **Achievements in Fiscal Year 2002**

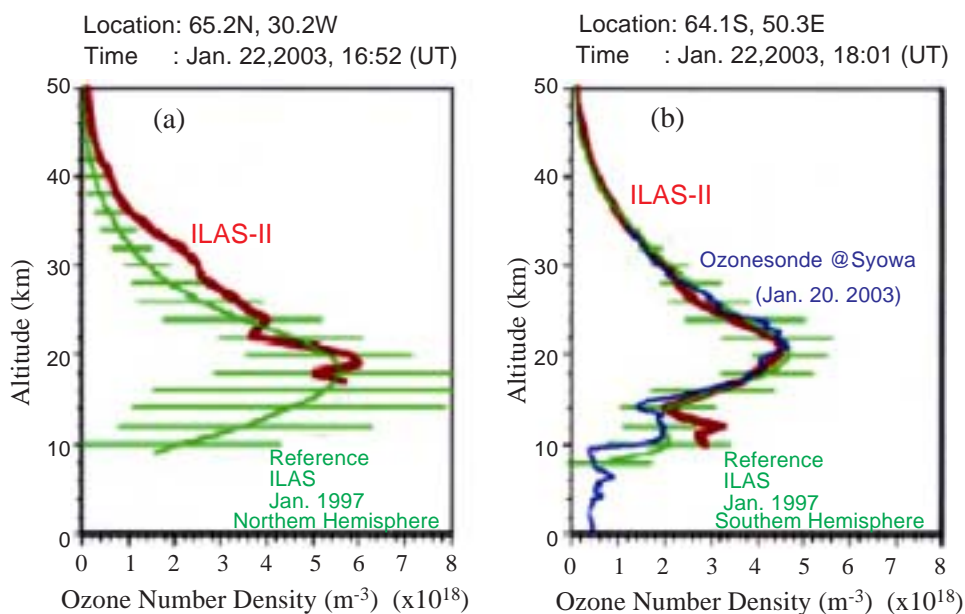
Vertical profiles of atmospheric constituents, such as ozone, water vapor, methane, nitrous oxide, nitric dioxide, and nitric dioxide were observed by the ILAS sensor. The data were processed with the version 5.2 retrieval algorithm and released to the public this fiscal year. The vertical profiles derived from the version 5.2 data were compared with those obtained by various remote-sensing techniques. For example, the vertical profiles of ozone concentration obtained by the version 5.2 algorithm were compared with those obtained by 3 foreign satellite-borne sensors: the version 19 Halogen Occultation Experiment (HALOE), version 6 Stratospheric Aerosol and Gas Experiment II (SAGE II), and version 6 Polar Ozone and Aerosol Measurement II (POAM II) algorithms. The agreement between ILAS ozone data and other satellite data was better than  $\pm 12\%$  for most scenarios between 21 and 50 km altitude, with the exception of January in the southern hemisphere at 41 to 50 km. ILAS version 5.2 ozone data were also compared with the vertical ozone profiles measured by ozonesondes, balloon- or aircraft-based instruments, and ground-based instruments. The agreement between ILAS and ozonesonde comparisons between 13 and 30 km was good (within  $\pm 10\%$ ) for both hemispheres. The ILAS ozone data also agreed within  $\pm 10\%$  with data from the balloon, aircraft-, and ground-based instruments between 9 and 50 km, with some exceptions. The validation study demonstrated that the version 5.2 ILAS ozone data were more accurate than the former, version 3.10, ILAS data. The validation of other chemical species was also studied.

ILAS-II onboard the Advanced Earth Observing Satellite-II (ADEOS-II) was successfully launched on 14 December 2002. ILAS-II Initial Checkout (ICO) was implemented between 20 and 23 January 2003. During ICO, some of the data measured by ILAS-II were processed and analyzed and the vertical profiles of the concentrations of ozone and other atmospheric trace species were retrieved. (Fig. 1) shows the vertical ozone profiles observed over Greenland at 16:52 UT on 22 January 2003 (Fig. 1(a)), and over Japan's Antarctic Syowa Station at 18:01 UT on the same day (Fig. 1(b)). The averages and ranges of fluctuation (3s) of data observed by ILAS for January 1997 are also shown, for comparison. The ozone profile observed by ozonesonde over Syowa station on 20 January 2003 is shown in Figure 1b. The ozone profiles derived from ILAS-II are in agreement with those observed by ILAS and by ozonesonde at altitudes higher than 15 km. (Fig. 1)

Ozone lidar data, which have been collected at Tsukuba since 1986, were re-analyzed with an improved algorithm. Systematic errors caused by background signals, signal-induced noises, and dead-time effects were successfully eliminated from the original return signals, then the quality of the detected signals was improved. Atmospheric

**Fig.1**

Vertical profiles of ozone concentration retrieved by analyzing ILAS-II data (red lines) collected on 22 January (a) at 16:52 UT over Greenland and (b) at 18:01 UT over Japan's Antarctic Syowa Station. The average values of data observed by ILAS in the same month in 1997 are also shown as reference values (green lines). The error bars indicated are 3 times the standard deviation. The ozonesonde observation was performed by the 43rd Japanese Antarctic Research Expedition at Syowa Station 2 days before the ILAS-II observation, and the result is shown in (b) by the blue line.



optical values and parameters, such as the ratio of aerosol extinction coefficient to backscattering coefficient, wavelength dependence, boundary altitudes, and atmospheric density were modified by changes in practical and temporal values after the comparison of lidar data with other supportive data from SAGE II, CIRA, NCEP, and radiosonde. We confirmed that the vertical profiles of the lidar ozone concentration agreed with those obtained by SAGE II within  $\pm 10\%$  in the range of 20 to 40 km altitude.

Because ILAS measurements provide vertical profiles of several chemical species, including  $O_3$ ,  $N_2O$ ,  $HNO_3$ , and  $NO_2$ , in the Arctic region in 1997, changes in ozone concentration were quantified on the basis of an  $N_2O$ - $O_3$  correlation using ILAS  $N_2O$  and  $O_3$  data. The quantified ozone changes were plotted against the amounts of  $HNO_3 + NO_2$ , which were calculated from ILAS data. We found that a rate of ozone loss of about 1 ppmv/month was maintained until the middle of April of 1997 for air masses with 5 to 7 ppbv  $NO_y$  (total oxides of nitrogen) content. Maximum ozone loss (1.4 ppmv/month) was observed at the 500-K of potential temperature level in mid-March, when the residual  $NO_y$  level was reduced to 8 ppbv, mainly because of denitrification. Detailed analyses of the data suggested that air masses with smaller  $NO_y$  content experienced greater ozone loss.

By using  $HNO_3$ - $N_2O$  and  $HNO_3$ - $O_3$  correlations derived from the ILAS data, we also evaluated the irreversible redistribution of  $HNO_3$  during the Arctic winter of 1996—1997. Denitrification and nitrification started just after the Arctic vortex had cooled to below the ice frost point ( $T_{ice}$ ). Trajectory analyses of the air masses observed by ILAS suggest that denitrification occurred only in the air masses that were once cooled to near  $T_{ice}$  and were kept at temperatures below the nitric acid trihydrate saturation threshold continuously for more than 4 days. A box model including polar stratospheric cloud formation, growth, and gravitational sedimentation processes was developed to clarify the mechanism of the denitrification process.

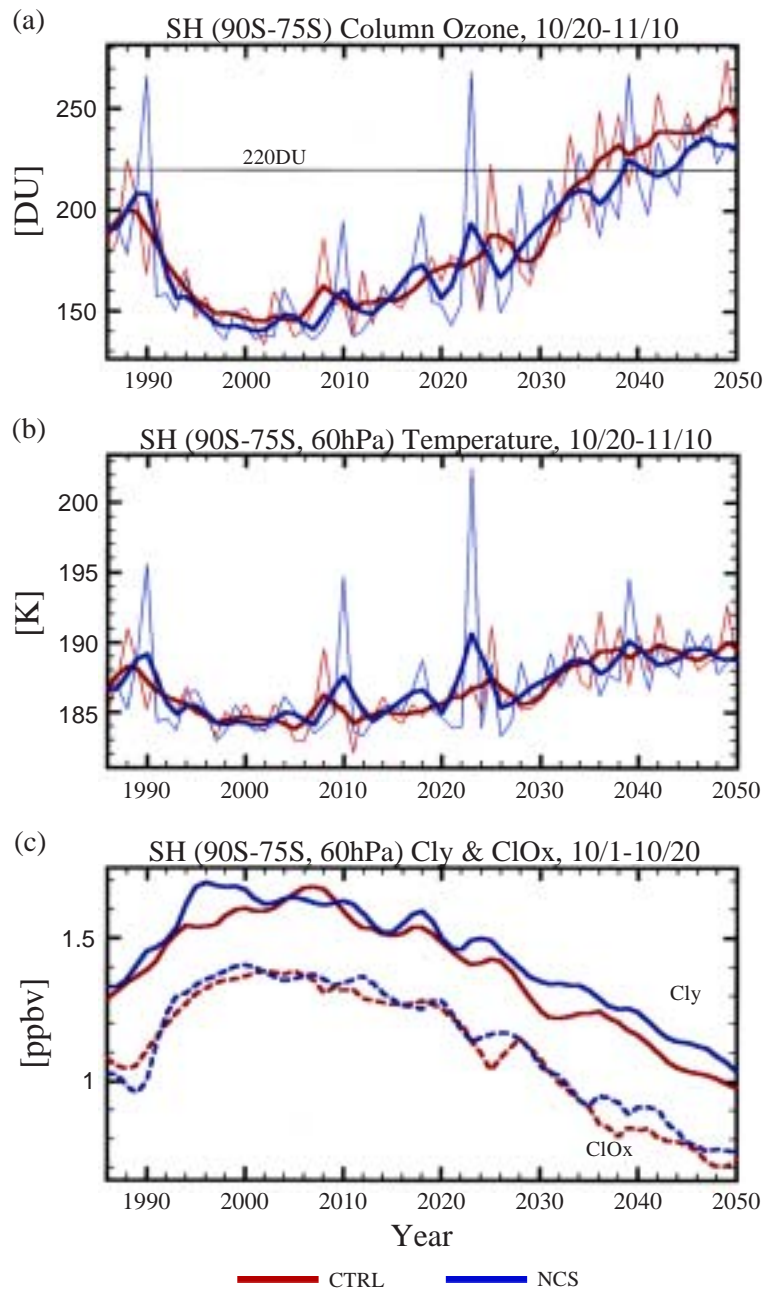
As a chemical climate model, we developed an atmospheric general circulation model with fully interactive stratospheric chemistry. We used the model to calculate the time—latitude cross-section of the zonal mean column ozone. We then compared the results of the calculation with the observed cross-section. Although the calculation overestimated the amount of ozone in the southern mid-latitudes and indicated a delayed appearance of the Antarctic ozone hole, it was capable of reasonable reproduction of our observations.

We used the chemical climate model to examine the numerical integration of ozone change against increasing CO<sub>2</sub> concentration. We performed 65-year model integrations for the evolution of 2 different scenarios from the same initial state, which was created by 22 years of integration for 1986 conditions. One of the integrations ('CTRL') was a control experiment that included the trends in concentration of halocarbons and those of all well-mixed greenhouse gases, such as CO<sub>2</sub>, CH<sub>4</sub>, and N<sub>2</sub>O, from 1986 to 2050. The other experiment ('NCS') studied the chlorine trend but the CO<sub>2</sub> concentration was not increased: instead, 1986 conditions for CO<sub>2</sub> were used throughout the integration. The results of the numerical integration are shown in (Fig. 2). The calculated column ozone level in the Southern Hemisphere polar region decreased at the same time as the ozone hole became smaller, between 1986 and 2000; the smallest value for column ozone (ca. 140 DU) appeared at around 2000. After 2000, the Antarctic springtime ozone level remained very low at about 150 DU, increased slightly until 2015, and then continued to recover steadily until the end of the integration. The long-term trend of column ozone calculated in the NCS experiment was similar to that in the CTRL experiment. This result indicates that the temporal evolution of ozone seems to be affected by increases in the simulated chlorine loading, not by CO<sub>2</sub> increase. (Fig. 2)

It is well known that a local total ozone minimum appears over the subtropical western Pacific in the Northern Hemisphere in winter. To examine the vertical structure of this ozone minimum, we analyzed vertical profiles of HALOE ozone data. The total ozone minimum was found to result from a minimum in the stratospheric ozone. We also found that the vertical profile of the ozone mixing ratio deviation from the zonal mean showed a bimodal structure: 1 minimum at around 20 km altitude and the other at around 30 km. Analysis with a simple photochemical transport model suggested that the low level of mid-stratospheric ozone is caused by southward transport of high-latitude ozone-poor air from the Arctic region, and that the ozone minimum in the lower stratosphere is caused by northward advection of ozone-poor air from the equatorial region. A nudging Chemical Transport Model (nudging CTM) developed at NIES was applied to simulate the total ozone minimum over the subtropical western Pacific in the northern hemisphere. The horizontal distribution of the observed ozone minimum was well simulated by the model. The vertical structure of the ozone mixing ratio deviation from the zonal mean was also calculated with the nudging CTM. The distinctive features of the vertical distribution—that is, the two negative deviations from the zonal mean—could be reproduced by the model.

**Fig.2**

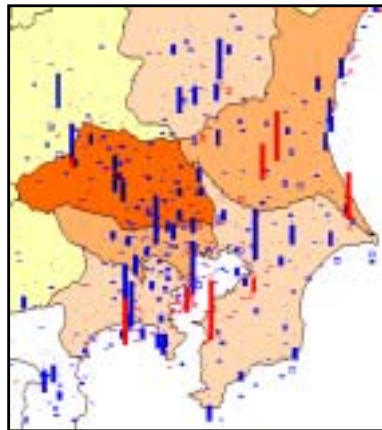
Simulated temporal evolution of various parameters averaged between 90° and 75° S. (a) Column ozone averaged between 20 October and 10 November; (b) Temperature at 60 hPa averaged over the same period; (c)  $\text{Cl}_y$  (continuous lines) and  $\text{ClO}_x$  (dotted lines) mixing ratio at 60 hPa, averaged for the period 1 to 20 October. Thick lines in (a) and (b) are 5-year moving averaged data, whereas the thin lines are data for individual years. All lines in (c) are 5-year moving averaged data. Red lines show the results of a control experiment that included the trends of halocarbons and those of all well-mixed greenhouse gases, such as  $\text{CO}_2$ ,  $\text{CH}_4$ , and  $\text{N}_2\text{O}$ , from 1986 to 2050. Blue lines present the results of a numerical experiment that included the chlorine trend; 1986 conditions for  $\text{CO}_2$  were used throughout this integration.



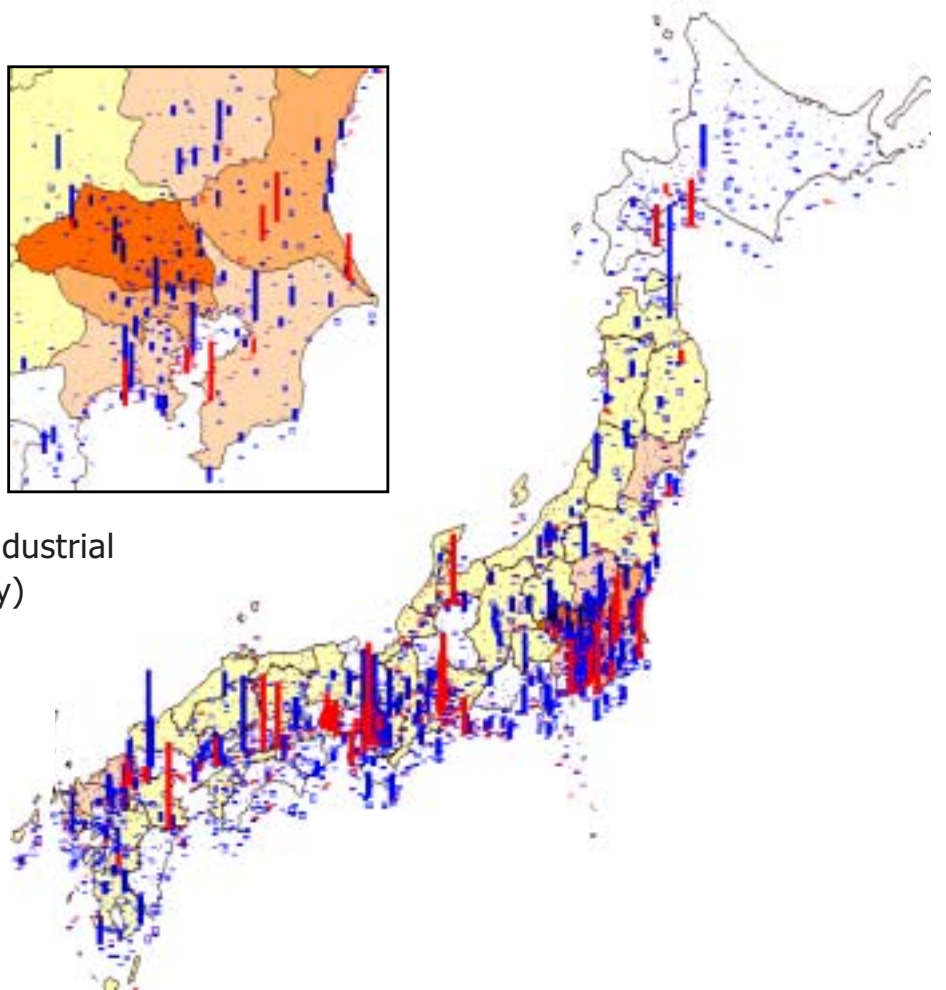
# Endocrine Disrupters and Dioxin Research Project

Emission from

Municipal Waste  
Incineration  
(pgTEQ/y)



Emission from Industrial  
Sectors (pgTEQ/y)



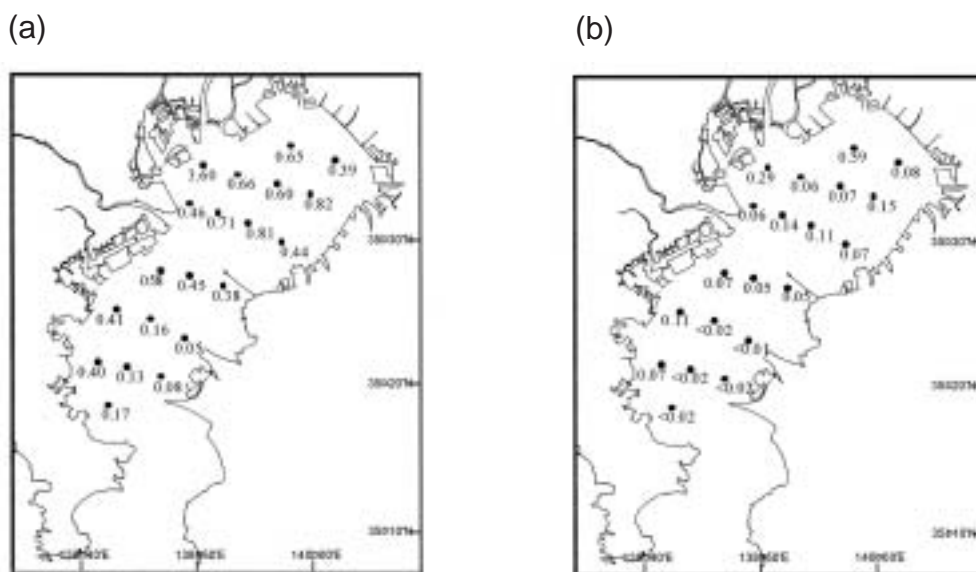
Geographical Distribution of Dioxin emission in Japan

The work of the Endocrine Disrupters and Dioxins Research Project, which utilizes NIES's new Endocrine Disrupter Research Facility and Specific Research Facility for Dioxins, has covered the following 4 themes: 1) development of methods for measurement and bioassay of these substances; 2) evaluation of the current status of environmental pollution; 3) hazard and effects assessments; and 4) development of countermeasures and integrated information technologies.

In FY 2002, we made major advancements in the following areas.

1) **Measurement of chemicals in environmental samples** was improved through the use of GC–NCI–MS and LC–ECD for non-volatile and thermally unstable compounds, and by the use of a GC–HRMS method to measure very low amounts of volatile compounds such as dioxins. We developed a LC–MS–MS method for the analysis of estrogens and their conjugates in sediment and water samples. We applied this improved method to water samples and surface sediments taken from Tokyo Bay to investigate the distribution of estrogens and their conjugates in the environment (Fig. 1).

**Fig. 1**  
(a)  
Distribution of estrone in surface sediment in Tokyo Bay (ng/g-dry).  
(b)  
Distribution of 17  $\beta$ -estradiol in surface sediment in Tokyo Bay (ng/g-dry).



We also improved our ability to detect 2, 3, 7, 8-TCDD by fine-tuning of our high resolution mass spectrometer and high volume injection for gas chromatography; this enabled us to assess human blood samples as small as 10 mL.

2) ***In vivo* and *in vitro* bioassays** are important methods of screening chemicals for their endocrine disrupting properties. We developed 7 *in vitro* assays, including yeast two-hybrid reporter-gene assays to assess estrogen, androgen and thyroid hormone

activity, as well as an ELISA-based assay for human estrogen receptor binding and for cell proliferation using neuronal cell lines. We showed that the receptors of different species have different affinities to chemicals: for example, the estrogen receptor  $\alpha$  of the freshwater fish medaka had higher sensitivity to the alkylphenols tested than did human estrogen receptor  $\alpha$  or  $\beta$ . We tested environmental samples and samples of industrial effluent by using a medaka estrogen receptor (ER) system, and found that many samples showed estrogenic activity by the medaka system but not the human ER system (Fig. 2).

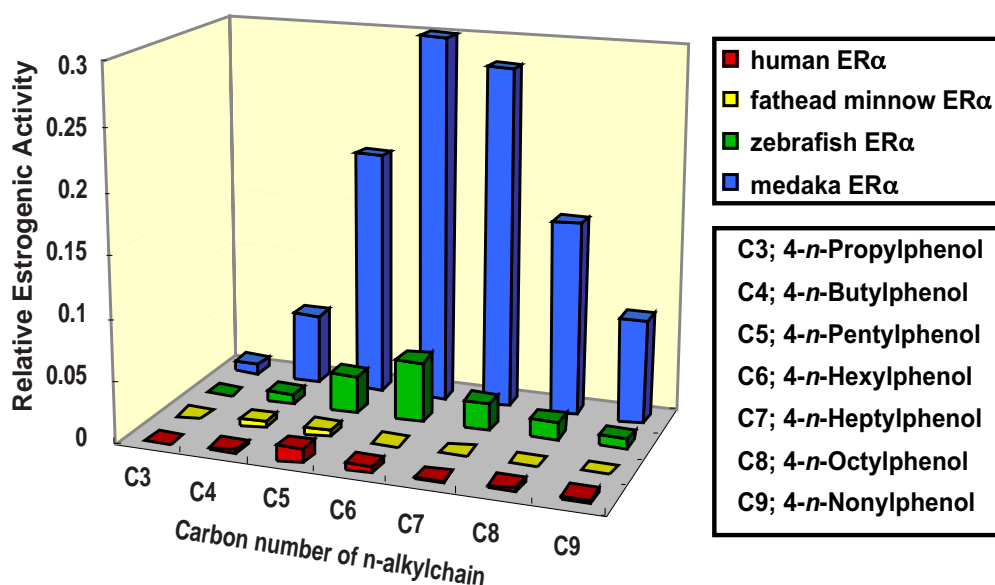


Fig. 2

We used *in vivo* assays in medaka to detect vitellogenin synthesis and to perform one-and-a-half generation tests. The small crustacean *Daphnia magna* is also used in our laboratory as a test animal to investigate the effects of endocrine disrupting chemicals on invertebrates. We found that the sex ratio of the offspring of *D. magna* was skewed dramatically toward males by exposure of mature adults to juvenile hormones and juvenile-hormone-mimicking pesticides. We also use *in vivo* testing of a frog (*Xenopus*) and reproduction and developmental toxicity tests in freshwater shrimp, chickens, freshwater mud snails, mice, and rats. The use of both *in vitro* and *in vivo* assays has enabled us to find several new compounds with estrogenic activity.

3) We have also been studying the **effects of EDCs on the neuro-brain system**. We have installed a high-field (4.7 T) magnetic resonance imaging (MRI) spectrometer for human study. We developed a method to obtain a 3-dimensional anatomical image of the human brain with 1 mm resolution at 4.7 T. Further,  $^1\text{H}$  and  $^{31}\text{P}$  spectra from an area of interest can be observed in 10 min, exhibiting glutamate (a representative

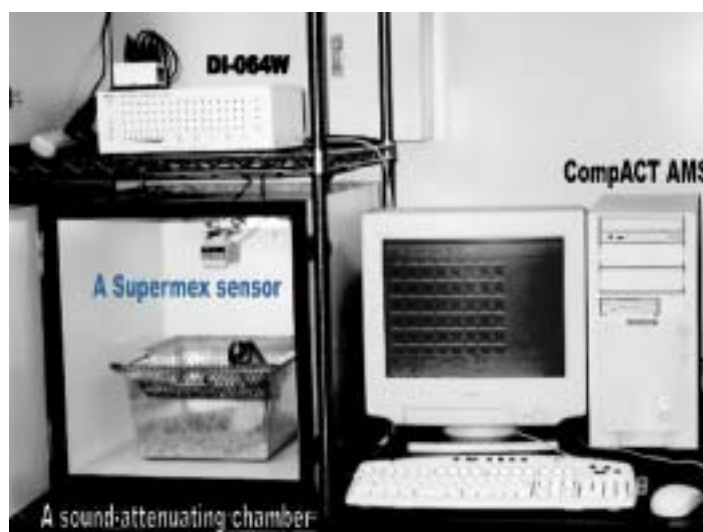
excitatory neurotransmitter) and ATP (an energy source for brain activity) in both human and rat brains.

To assess the effect of EDCs on the nervous system and behavior, we observed the effects of bisphenol-A (an endocrine disrupter), ethylenethiourea, and other positive controls on experimental animals. Treatment with the organotin neurotoxicant trimethyltin (TMT) induced reactive astrocytosis in the rat hippocampus, as evidenced by the results of vimentin immunohistochemistry; the effects were profoundly exacerbated by adrenalectomy. Prolonged administration of dexamethasone (a type II glucocorticoid receptor agonist) not only attenuated the exacerbating effects of adrenalectomy but also partly reversed the TMT-induced neuronal loss and reactive astrocytosis.

Intracisternal administration of bisphenol A in 5-day-old Wistar rats caused hyperactivity at 4–5 weeks of age. These rats were about 1.6 times more hyperactive than vehicle-treated rats in the nocturnal phase (Fig. 3).

**Fig. 3**

The Supermex system. The general view of a system consisting of a sound-attenuating chamber, a Supermex sensor, a rat in the home cage, a 64-channel interface (DI-064W), and a personal computer with CompACT AMS software.



We compared the relative impacts of in utero versus lactational exposure to TCDD on serum thyroxine (T4) levels by using a cross-fostering protocol in Holtzman rats. The T4-suppressing effects of TCDD on postnatal day 21 were mainly due to lactational rather than in utero exposure, and we suggested that these effects were caused by enhanced biliary excretion of T4-glucuronide through induction of UDP-glucuronosyltransferase (UGT-1), a TCDD-inducible enzyme.

Novel TCDD-responsive genes were sought among those responsive to estrogen, using DNA microarrays spotted with estrogen-responsive genes. We verified 23 genes up- or down-regulated by TCDD exposure in MCF-7 cells and 14 genes in RL95–2 cells.

4) To determine the **effects of EDCs on wildlife**, we observed sea snails and bivalves along the Japanese coast. Some species of snail now face reproductive toxicity from organotin compounds. We collected abalone (*Haliotis gigantea*) specimens from 32 coastal sites to examine tissue concentrations of organotin compounds and search for histological abnormalities in the gonads. Laboratory flow-through exposure experiments with TBT were also conducted in abalone to evaluate ovarian spermatogenesis in a dose-dependent manner. We also carried out preliminary evaluation of the reproductive success of abalone exposed to organotin, from the results of *in situ* reproductive experiments on adult abalone; laboratory toxicity tests on fertilized eggs and larvae; and field observations of the distribution, settlement, and growth of larvae.

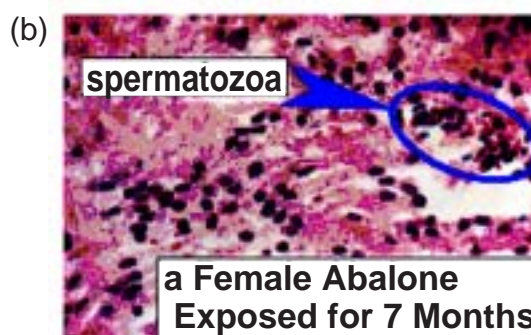
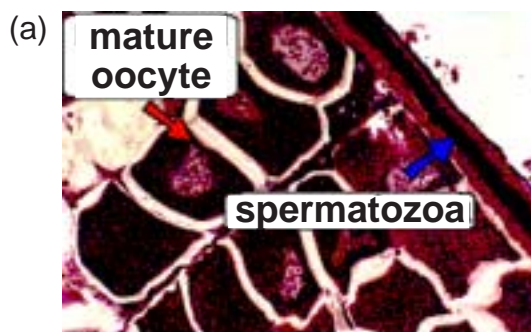
In October 2002 we began another field study to search for endocrine disruption in marine fish in Tokyo Bay. We selected the mud dab (*Pleuronectes yokohamae*) as a target species. We have analyzed its population dynamics, measured vitellogenin and steroid hormones in the plasma, histologically examined the gonads, and evaluated the presence of estrogenic compounds and other endocrine disrupters in the tissues (Fig. 4).

**Fig. 4**

(a) Ovarian spermatogenesis observed in giant abalone, *Haliotis madaka*, collected from an organotin-contaminated site in April 1996.

(b) Results of *in situ* exposure experiments near a shipyard for 7 months, using abalone (*Haliotis gigantea*) from a reference site.

Ovarian spermatogenesis was observed in approximately 90% of females. We also observed marked accumulation of organotin (tributyltin and triphenyltin) in the muscle of abalone exposed to organotin-contaminated seawater at the site for 7 months (June 1998 to January 1999).



We also examined fish and freshwater snails in Lake Kasumigaura, and we sampled seabirds for thyroid dysfunction.

5) To **reduce the emission of dioxins and prevent secondary emission to the environment**, we studied a method of monitoring and decomposing dioxins. We compared simple and rapid analytical methods, including a bioassay, and designed real-time monitoring equipment. To construct a system for identifying the source(s) of dioxins, we first categorized sources and environmental samples by a principal component analysis (PCA) based on their own homologue profiles. Pretreatment of data was required before we were able to determine that PCA and statistical standardization were the best methods. The use of 2,3,7,8-position chlorine-substituted homologues of PCDD/Fs and 1,2,3,4,6,7,9-HpCDD explained the differences among samples well. As a method of decomposing dioxins we trialed the use of ultrasonic irradiation. We also studied biological decomposition or inactivation of EDCs by using plant and soil bacteria.

6) Development of **integrated risk assessment and management of endocrine disrupting chemicals and other contaminants** by comprehensive integration of information and methodologies into an assessment scheme is a major objective of our team. A basis of this project is the “virtual world” geographic information system (GIS) framework, which has been developed since FY 1996 by an ad-hoc project team to manage the new interdisciplinary area of risk assessment and management of various chemicals at local and regional levels.

The FY 2002 study continued the efforts from FY2001, including development of an environmental-fate-modeling methodology, system and databases; development of emission inventory modeling methodologies; and statistical/geographic analysis of monitoring data. A grid-catchment integrated modeling system (G-CIEMS), a multimedia fate model for geo-referenced and spatially resolved fate simulation on a GIS system, was developed for the entire Japanese land environment and the surrounding ocean. A case study of dioxins was conducted over thirty-eight thousand  $5 \times 5$  km air grid cells, covering 38 000 catchments and river segments with 7 land-use categories, a river-networking database, and tentative sea compartments. The model can predict averaged environmental concentrations to within a factor of 2–3, a result that is a great improvement on existing multimedia fate modeling techniques.

We also prepared a database of EDCs; it is available through the web.

# Biodiversity Conservation Research Project

---



**left: Ponds having lots of  
Odonata species  
right: Ponds only a few  
species of Odonata  
inhabit**

The recent rapid expansion of human activity worldwide has resulted in continuing degradation of wildlife habitats and loss of biological diversity. In addition, ecological disruption by incursion of invasive species and production and release of genetically modified organisms has become a new problem. In the Biodiversity Conservation Research Project, which is composed of the 5 research teams described below, we are developing methodologies to assess changes in biodiversity on a variety of spatial scales, and are researching the ecological disruption caused by invasive species and genetically modified organisms.

### Wildlife Population Research Team

As the need to prevent the extinction of wild species is increasing, the Wildlife Population Research Team has been researching the mechanisms of population colonization and extinction, which comprise the process of species persistence. Dispersal of individual organisms is occurring between populations and may be influencing the viability and genetic uniqueness of each population. One of our interests is to study how populations are connected. In this fiscal year, we found that numbers of a threatened bird species, the Japanese marsh warbler (*Megalurus pryeri*), are increasing in one of a few remnant populations that are dispersed but interconnected within eastern Japan. Another focus is to incorporate our knowledge of the mechanisms of population connection into regional-scale plans for the conservation of population networks. We found that Japanese populations of a threatened freshwater fish, the three spine stickleback (*Gasterosteus aculeatus*), have maintained their well defined genetic diversity, which was formed in the historical course of population colonization (including artificial introduction) and extinction (Fig. 1). This genetic diversity is worth preserving from the point of view of restoration and transplantation of populations.

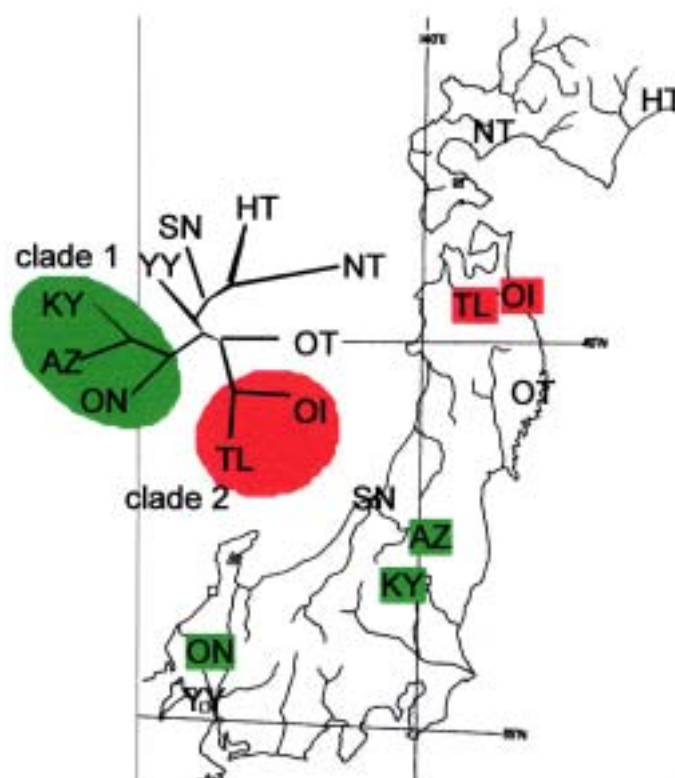
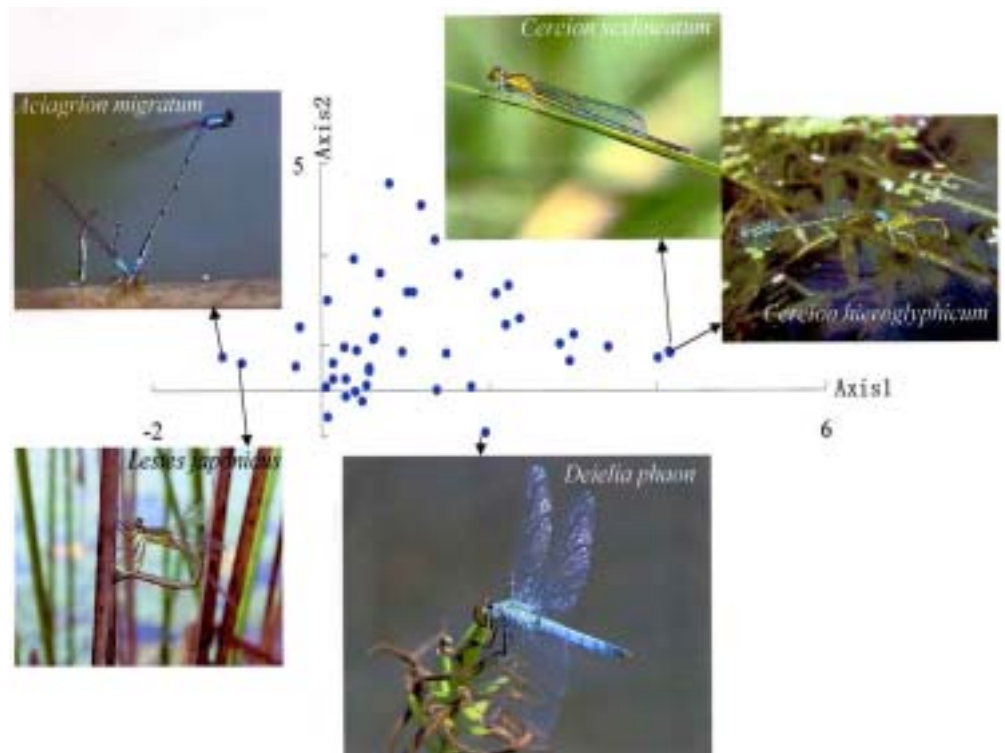


**Fig. 1**  
Genetic relatedness among 10 Japanese populations of a freshwater fish, the three-spined stickleback *Gasterosteus aculeatus*. Two genetically defined groups (clades 1 and 2) were recognized.

**Fig. 2**  
Detrended correspondence analysis ordinations of 45 species of Odonata in ponds. (Photographs: Takashi Aoki) *Aciagrion migratum* and *Deilelia phaon*, located at the left extremity of axis 1, prefer forests, whereas *Cercion hieroglyphicum* and *C. sexlineatum*, located at the right extremity of axis 1, prefer the flatter and warmer environment of paddy fields. *Lestes japonicus*, located at the lower extremity of axis 2, needs aquatic vegetation.



### Ecological Landscape Research Team

The Ecological Landscape Research Team explores the patterns of landscapes and their relationship to species diversity in aquatic ecosystems. We investigated the factors that regulate dragonfly and damselfly (Odonata) communities in a number of small agricultural ponds in Hyogo Prefecture, Japan. Multiple regression analysis showed that over 81% of the variation in richness of Odonata species inhabiting these ponds could be explained by 4 variables: the species richness of aquatic plants in the ponds; the presence of a forested area within a 200 m radius of the pond; the length of pond perimeter not covered by concrete edging; and the concentration of nitrogen in the pond water. Ordination by detrended correspondence analysis of 45 species (Fig. 2) revealed that the 2 most explanatory axes were closely related to species-specific voltinism and breeding organs. The positive significantly correlated environmental variable selected by axis 1 was the presence of a forested area within a 200 m radius of the pond, and the negative ones were the presence of a paddy field within a 200 m radius of the pond and the index of solar radiation. Those selected by axis 2 were a number of variables related to aquatic vegetation. Our results revealed some key properties of habitat selection by Odonata, as well as important environmental elements for the conservation of Odonata in these ponds.

We also examined the effects of habitat fragmentation on fish species richness on Hokkaido, the northernmost island of Japan.

### Biological Invasion Research Team

The Biological Invasion Research Team investigated the ecological impact of an “insect industry”, the commercial production of stag beetles. The breeding of these beetles has boomed in recent years in Japan. Many native and exotic species of stag beetle are now sold throughout Japan as pets (Fig. 3).

**Fig. 3**  
A stag beetle, *Dorcus titanus*, collected from Fuji City, Shizuoka Prefecture, Japan. It possessed the *mtDNA* haplotype of a Thai strain.



This commercialization is expected to have serious ecological impacts on the biodiversity of native stag beetles. Potential impacts are the destruction of natural populations in their native habitats, competition between native and exotic species, and alien parasite invasion. We focused on genetic disturbance as one of the ecological risks posed by this insect industry.

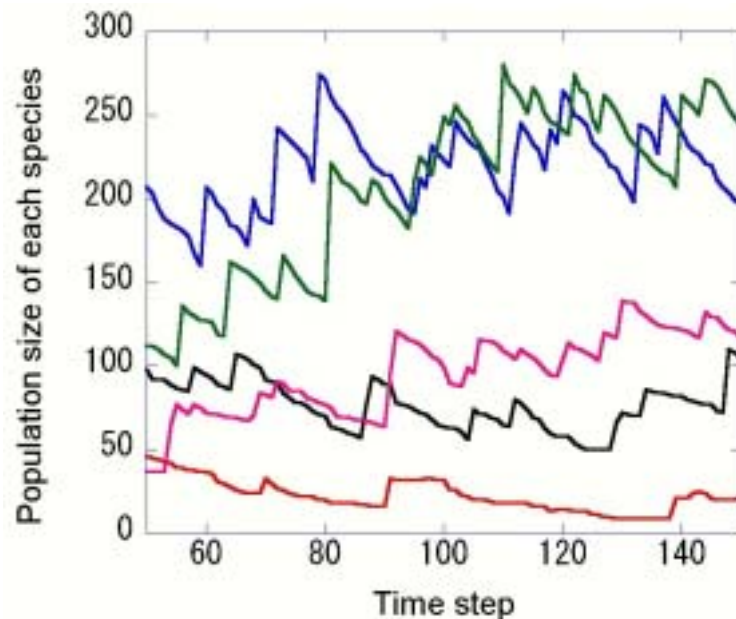
We investigated variations in the nucleotide sequence of *mtDNA* in Japanese and exotic *Dorcus titanus* stag beetles. Our aim was to determine the genetic differences between exotic and native beetles of this species and thus to assess the need to protect the genetic integrity of local beetle populations. Our results revealed that some of the Japanese individuals collected in the field had originated from exotic beetles. Commercialization of stag beetles has caused introgression of the genes of exotic beetles into Japanese beetle populations.

### Community Dynamics Research Team

The biodiversity of a forest ecosystem relies largely on the diversity of tree species. The coexistence of tree species is apparently paradoxical, because all species are competing for the same resources—namely, light, water, and nutrients. The reason why the most competitive species do not exclude others has been sought for a long time. Numerous hypotheses on the mechanism of tree species' coexistence within a forest have been proposed. One of them is the temporal fluctuation of reproduction, that is, the concept that species coexistence of sessile organisms competing for space is promoted if each organism produces offspring more than once in its life, and this reproduction is synchronous within each species but asynchronous among species. A minority species may recover its population size when it produces offspring and the other species do not. Available open spaces are then occupied by the minority species.

**Fig. 4**

Temporal change of population size of tree species within a simulation model of forest dynamics. Different lines represent different species. Abrupt rises in the population size occur in seed-production years. These rises are especially pronounced when the random reproduction events of a particular species do not overlap with those of other species, and the reproducing species can therefore monopolize vacant spaces.



In 2002, we tested the validity of this hypothesis as a mechanism for promoting species coexistence in a forest. We developed a spatially explicit simulation model of forest dynamics and used it to investigate the dynamics of species composition (Fig. 4). In the model, the density of dispersed seeds decreased with distance from the parent tree. We found that limited seed dispersal around parent trees enhanced species coexistence. The shorter the dispersal range, the greater the number of species that coexisted. Limited seed dispersal increases the probability that the offspring of minority species will be able to occupy open space in the absence of offspring of dominant species.

#### Biotechnology Risk Assessment Team

Genetically modified or “transgenic” plants have been generated and utilized for a variety of purposes, and there is public concern over their potential effects on the natural environment. A satisfactory method of evaluating and monitoring these effects needs to be established. *Glycine soja* is a Japanese domestic soybean and is widespread in Japanese soybean fields. Cultivation of transgenic soybean will bring about hybrids of *G. soja* and transgenic soybean (Fig. 5). We constructed F1 hybrids of soybean and *G. soja* and evaluated their phenotype and the stability of the transgene.

To monitor the fate of genetically engineered microorganisms introduced into the environment, we constructed a genetically engineered soil bacterium possessing a specific marker gene, the mercury resistance operon. This marker was maintained stably in host cells and proved to be a useful, easily detected tool. *Pseudomonas putida* PpY101/pSR134 containing the marker gene was introduced into an aquatic microcosm. We found that the numbers of this bacterium decreased more rapidly under light than in the dark.

In response to unsuitable environmental conditions, bacteria will change their metabolic and cellular components and enter a non-growth stage (VBNC; viable but non-culturable). To confirm this phenomenon, we isolated 5 strains from a municipal sewage disposal plant and stressed them by chlorination. Four strains became VBNC, suggesting that the VBNC stage is common, and that we need a new system for determining whether such bacteria are living or dead.



**Fig. 5**  
F1 hybrid constructed from *Glycine soja* and transgenic soybean .  
Left: *Glycine soja* plant and seeds. Middle: F1-hybrid plant and seeds.  
Right: transgenic soybean plant and seeds.



*Glycine soja*

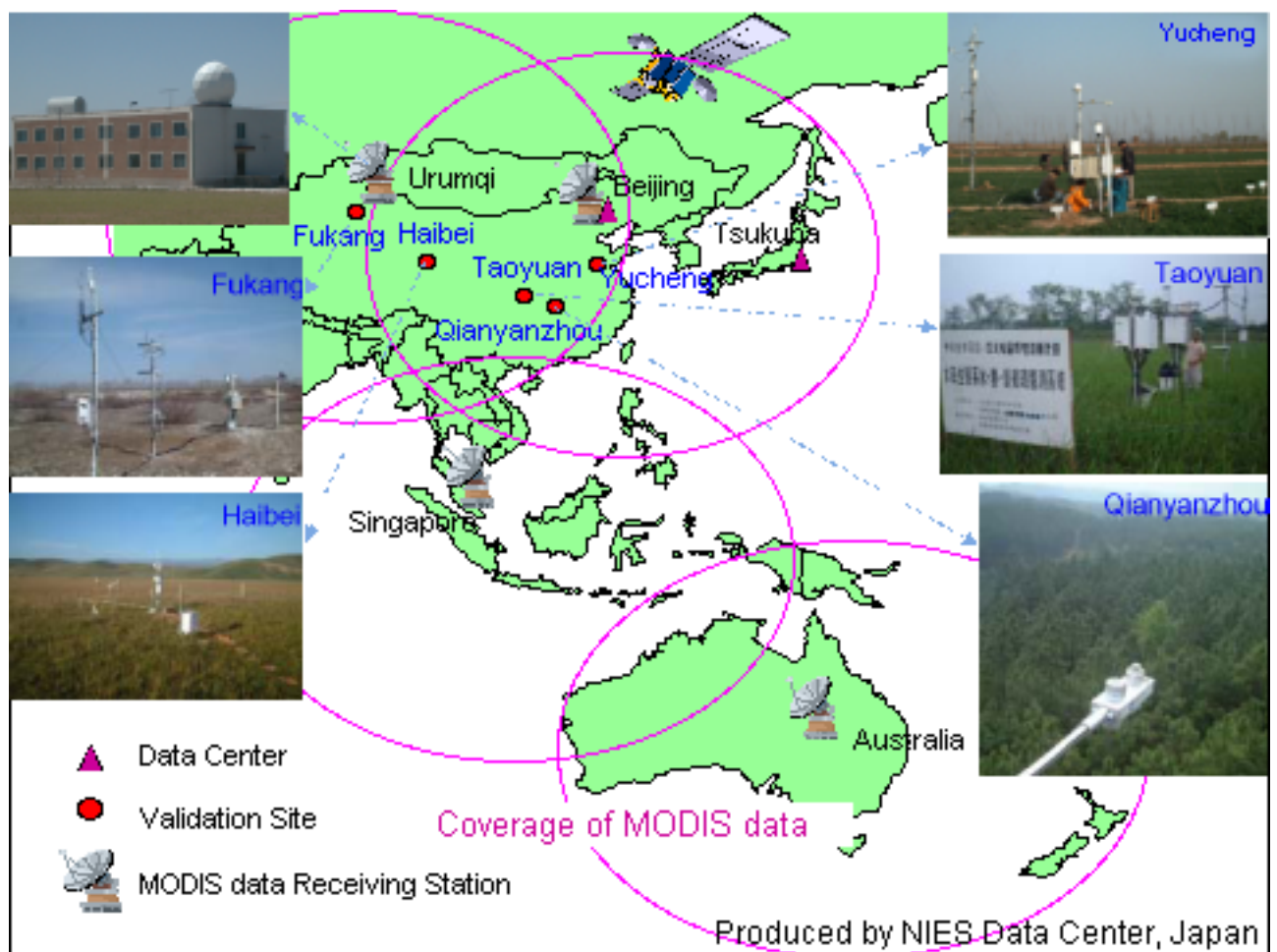


F1-hybrid



transgenic soybean

# Watershed Environments and Management Research Project



### **Objectives**

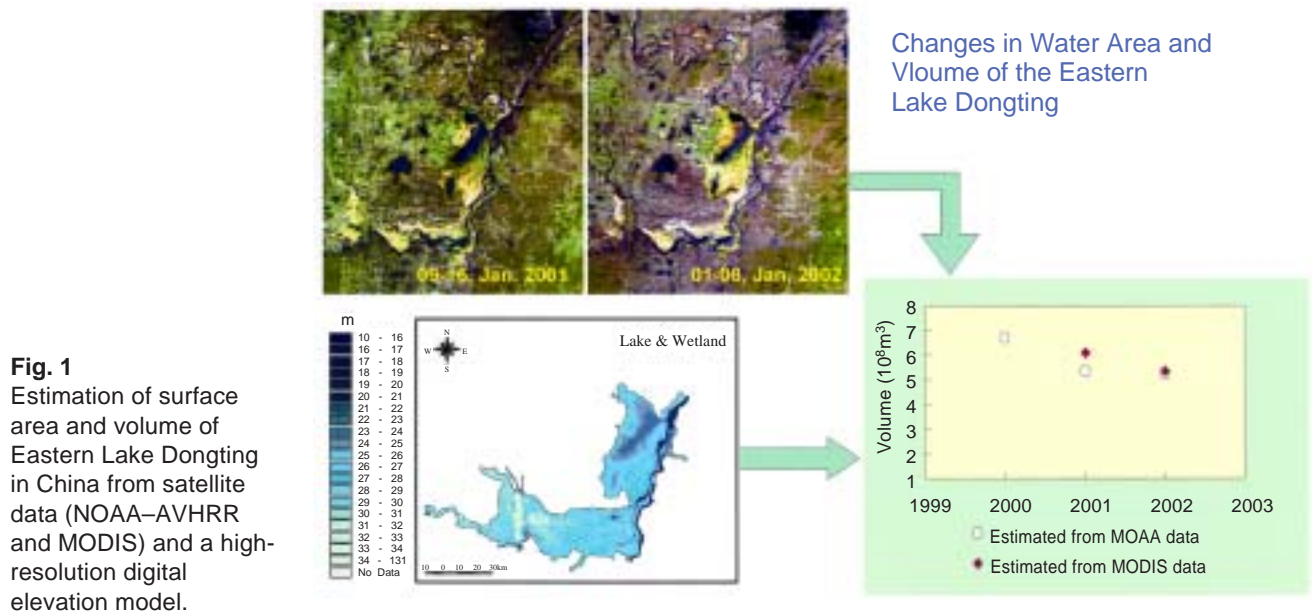
Environmental conditions are deteriorating in the Asia-Pacific region, home to about 60% of the world's population and currently experiencing rapid population and economic growth. The fact that many countries in the region are at different stages of economic development creates a complex set of problems that seriously constrain balanced and sustainable economic development. Examples are the health impacts of industrial pollution, degradation of natural resources through industrial development, increased pollution associated with greater use of motor vehicles and the concentration of populations in cities, and increased greenhouse gas emissions. In the context of the major economic growth in Asia in the twenty-first century, we must give thought to sustainable methods of managing the environment that take into account the ecosystem functions that govern the cycle of nature. Our research will focus on the circulation of water and materials in East Asia; we will be working to scientifically observe and understand the ecosystem functions of major river basins in China, the heart of the region. In addition to developing methods to forecast the degradation and recovery of ecosystem functions through models that manage the river basin environment on the basis of ecosystem function, we will propose sustainable environmental management plans that cover the application of environmental recovery technologies, the re-evaluation of development plans, and the reduction environmental loadings.

### **Monitoring of disasters and environmental degradation**

If we are to take effective countermeasures against such environmental depletion and degradation we will need to examine the present environmental conditions and changes in natural resources. As one step toward solving these problems, the National Institute for Environmental Studies (NIES) in Japan and the Institute for Geographical Sciences and Natural Resources Research (IGSNRR) of the Chinese Academy of Science have carried out collaborative research to develop an integrated environmental monitoring network system which, since the formal participation of Singapore and Australia, has now expanded to cover the entire Asia-Pacific Region. The data-analysis centers at IGSNRR and NIES store a database that includes satellite data (e.g. MODIS, LANDSAT, ASTER, NOAA, TRMM), geographic information system (GIS) data, and measurements from ground-truth ecological stations.

### **Monitoring of disasters and environmental degradation**

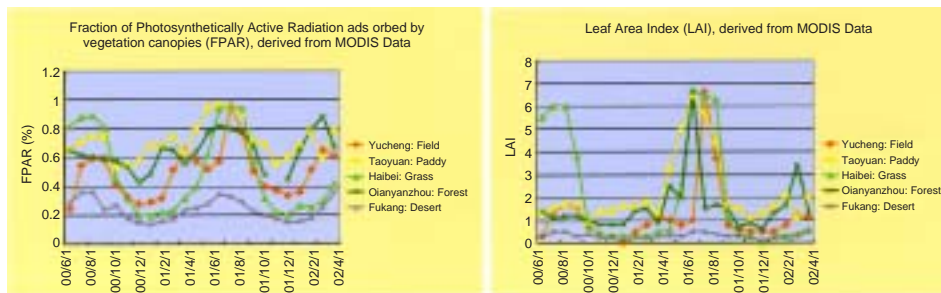
In eastern Asia, serious disasters occur frequently on large regional scales owing to environmental degradation. For example, dust storms now occur on a larger scale, and the damage they cause increases each year. Meanwhile, desertification and grassland degradation are becoming more severe, thanks to human-driven factors such as overcultivation, overgrazing, exploitation and misuse of water resources. Satellite observation is a tool that can help us to monitor these phenomena over time. Spatially wide and temporally long observations by satellite data enable us not only to monitor natural disasters, but also to detect the land use and land cover changes that occur as a result of human activities. The integrated monitoring network estimated the surface area and volume of Eastern Lake Dongting in eastern China with NOAA-AVHRR and MODIS data coupled with a digital elevation model (see Fig. 1).



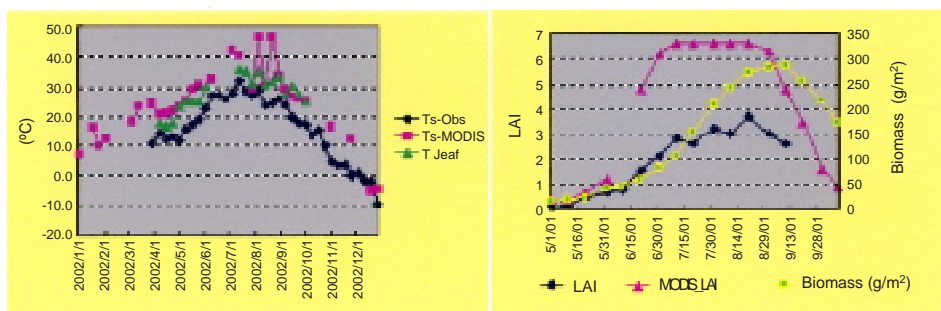
### Development of a data-processing system for the derivation of environmental indices and its validation from ground-truth data

At the NIES data center we have already improved a data-analysis system based on an algorithm that NASA has developed, and we now produce the following high-order land products of MODIS: surface reflectance, land surface temperature (LST) and emissivity, land cover and land cover change, vegetation indices, thermal anomalies, fires and biomass burning, leaf area index (LAI) and fraction of photosynthetically active radiation absorbed by vegetation (FPAR), net photosynthesis (PSN), and net primary productivity (NPP). Although we can produce MODIS high-order products by a data processing system, most of them have not yet been calibrated or validated by ground-truth data in various ecological systems. (Fig. 2(a)) shows the annual changes in FPAR and LAI at each of the 5 validation stations listed below, and (Fig. 2(b)) shows the results of validation; such comparisons indicate that the MODIS products must be validated before they are put into use.

To validate satellite remote-sensing data, in 2002 we established a ground-truth observation network through which long-term measurements of water vapor, energy exchange, and carbon dioxide from a variety of ecosystems—at Haibei (grassland), Yucheng (irrigated fields), Taoyuan (paddy fields), Qianyanzhou (forest), and Fukang (desert) in China—are measured and integrated into a consistent, quality-assured, and documented dataset. The dataset includes micrometeorological factors, eddy covariance fluxes, vegetation characteristics, and soil physical and chemical properties. An example of the observed heat, water, and  $\text{CO}_2$  fluxes at Yucheng Station in 2002 is shown in (Fig. 2(c)). Clearly, marked  $\text{CO}_2$  absorption and  $\text{H}_2\text{O}$  evapotranspiration occurred during the crop growth season.



(a) Annual changes in fraction of photosynthetically active radiation absorbed by vegetation canopies (FPAR) and leaf area index (LAI) derived from MODIS data at five validation sites



(b) Comparison between observed land surface temperature (left: Yucheng site), and leaf area index (LAI) (right: Haibei Site) with MODIS products in 2001

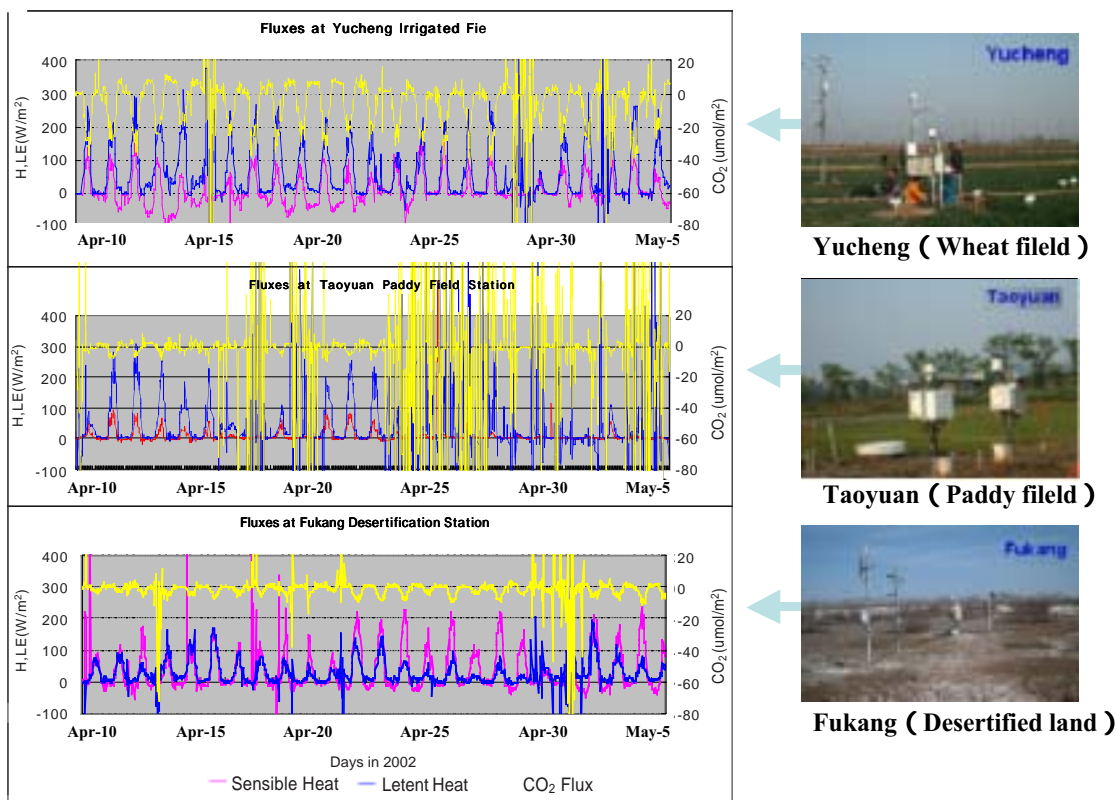


**Fig. 2** Results and their validation by the integrated monitoring network.

(c) Examples of observed data at each ecological station in China

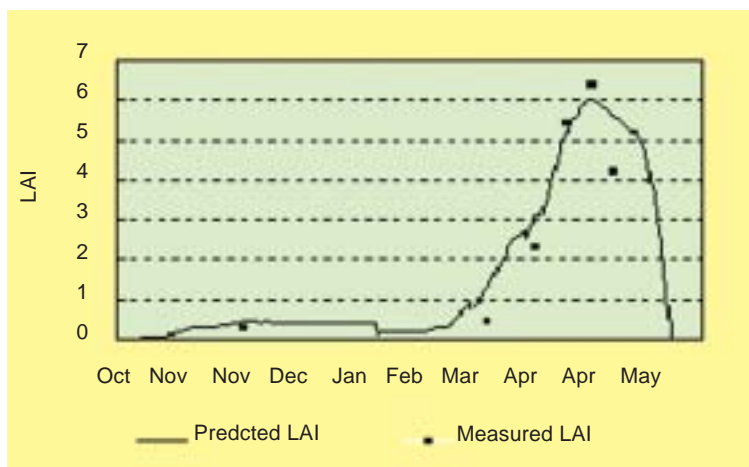
### **Optimum irrigation management on the North China Plain**

To achieve sustainable agriculture, we must manage optimum water use for cropping, and we must understand the relationship between vegetation growth and water consumption. A sophisticated Decision Support System for Agro-technology Transfer (DSSAT) model has been used to simulate agricultural production.

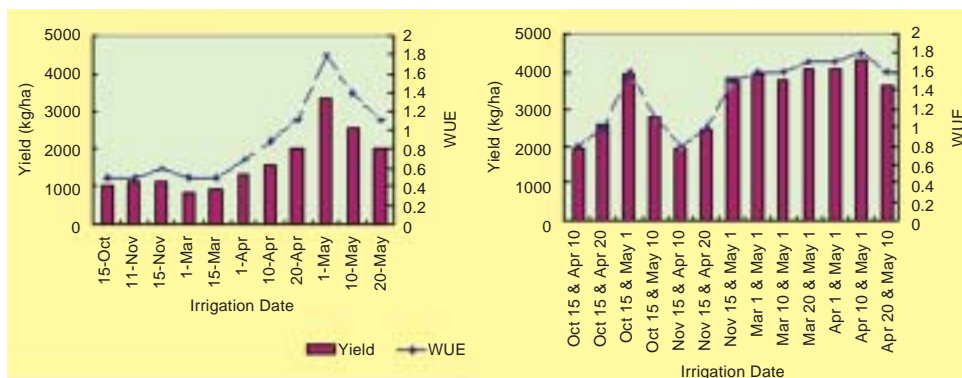
A simulation was applied to wheat production on the North China Plain, one of the largest bases of crop production in China. The widely distributed irrigation networks rely on the use of groundwater, and this has caused a rapid decline in the water table in the region. It is reported that the groundwater level dropped 19.7 m over a 28-year period from 1974–2001 in Gaocheng County. Groundwater drawdown takes place mainly in March–June, which coincides with the wheat-growing season. Sustainable development of agriculture in this area is facing huge challenges. In such areas, it is very important for us to determine the best irrigation scheme for decreasing the amount of water used for irrigation. Our strategy is to produce the highest or near-highest yield with the smallest amount of irrigation water through the improvement of water use efficiency (WUE).

The model can simulate, in daily steps, wheat phenological development from planting through to germination, maturity and harvest; photosynthesis and plant growth; carbon allocation to the root, stem, leaf, and grains; and soil water and nutrient movement. To test the validity of the model in the study region, experimental data from the 2000–2001 wheat-growing seasons were used. Comparisons of the simulation results and the measured results for LAI of wheat in Gaocheng County are shown in (Fig. 3(a)); they indicate that the model simulation is acceptable in the study region for winter wheat management.

The simulation results indicate that this model is a strong tool for determining the wise use of ecological goods and services, such as freshwater resources (irrigation) for crop production. It can provide information on the amount and timing of irrigation to produce the highest crop yield. For example, we determined the optimum timing of irrigation with the same amount of water applied as either 1 or 2 irrigations (Fig. 3(b)). According to the simulation, the highest yield from a single irrigation was achieved by irrigating on 1 May, but an even higher yield, and thus greater WUE, was achieved by dividing the water resource into 2 irrigations, on 10 April and 1 May. Through scientific irrigation scheduling, WUE can be improved and irrigation water can be saved while maintaining a high wheat yield.



(a) Measured and simulated leaf area index (LAI) of wheat in Gaocheng County, China



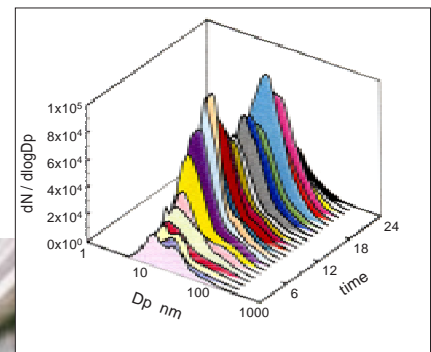
(b) Results of DSSAT model simulation of wheat yield and water use efficiency with one or two irrigations in Gaocheng County, China

**Fig. 3**  
Application of optimum management of agricultural water-use.

# PM<sub>2.5</sub> & DEP Research Project



Roadside site



Size distribution observed



Measurement equipments

Observation of ultra fine particles at a roadside atmosphere

### **Environmental fate and risk assessment of fine particulates and diesel exhaust particles**

Air pollution from vehicle emissions remains a serious problem in urban areas. The PM2.5 and DEP Research Project Group is carrying out investigations to better understand the characteristics of pollution sources as well as the environmental fate of fine particulate matter (PM<sub>2.5</sub>) and diesel exhaust particles (DEP) and their effects on human health.

### **Independent Senior Researcher**

An independent senior researcher began a 3-year interdepartmental project on approaches to reducing the air pollution caused by diesel vehicles along heavily trafficked urban roads. Reduction strategies studied were: (1) enhancement of the diffusion of exhaust around roads by changing the roadside environment; and (2) improvement of fuel and thus reduction of the toxicity of diesel exhaust. Several PM2.5 & DEP Research Project members conducted wind tunnel experiments and field surveys in relation to strategy (1). They made progress in the first year of the project, FY 2002, as follows.

The wind tunnel experiments were performed on a 2-dimensional 1:300 scale model of a real built-up area in Ikegami-Shinmachi, Kawasaki, where a heavily trafficked roadway runs at ground level below an elevated parallel road. We studied the flow and distribution of air pollutants around the roadway and the lid effect of the elevated road on pollution. We then studied the effects of structural changes to the roads and the surrounding environment on pollution levels. We also studied the effect of thermal stratification on pollution in the area and found that it greatly increased the pollution at the roadside and in its surrounding area. We obtained several suggestions for reduction of pollution. Further, in the wind tunnel experiment, we succeeded by the PIV (particulate image velocimetry) method (see Fig. 1) in observing an instantaneous 2-dimensional velocity distribution of air in a cross-section perpendicular to the road and the elevated road. We now have a tool to study transient states in addition to mean states.

We also conducted 2 field surveys in Kawasaki to measure the real spatial distribution of particulate matter (PM) and NO<sub>2</sub> around the crossing. These results will be compared with those of the wind tunnel experiments and numerical simulations. For particulates 1.0–10 μm in size, we developed sensing units from LED (light emitting diode) dust sensors. We distributed the sensing units at about 30 points around the crossing and measured the particulate density at these points simultaneously every 1–10 min. In addition, we measured the numbers of particulates over 0.03–1 μm that had accumulated. The densities of particulates of both size ranges diminished quickly with increasing distance from the road. This fact suggests that upward diffusion plays a key role, and we are now seeking ways to promote upward diffusion.

field surveys near trunk roads, compiled emission inventories, reviewed technical and regulatory measures, and developed GIS-based tools for assessing traffic pollution. In fiscal year 2002, particulate and gaseous pollutants from diesel-engine vehicles were measured on the chassis dynamometer as well as by on-board equipment to examine emission factors under various realistic driving conditions. Changes in the size distribution and concentration of particles after emission were observed in a dispersion chamber. Field measurements focusing on the size distribution of ultra-fine particles were undertaken at roadside sites under various traffic conditions. We found that heavy-duty vehicles were the greatest contributors of particles under 50 nm in diameter. We also designed the framework of a GIS-based integrated system for assessing the effectiveness of various policy measures: it consists of numerical models of traffic flow, particulate emission and dispersion, and exposure assessment. In particular, the integration of a dynamic traffic flow simulation model into the system was examined to assess the effectiveness of traffic demand management policies.

### Urban Air Quality Research Team

The Urban Air Quality Research Team has been investigating the relationships between changes in the relative importance of various air pollution sources and the spatial and temporal distribution of urban air pollution. To clarify the behavior of airborne particulates – such as PM<sub>2.5</sub> and DEP – and combinations of gaseous air pollutants, we have been conducting wind tunnel experiments, field observations, data analyses, and computer model simulations. In fiscal year 2002, we performed a series of thermally stratified wind tunnel studies, focusing mainly on air pollution distribution around the road overpass in Kawasaki, to determine the dynamic behavior of air pollution near roadsides. From 3-dimensional field observations, monitoring of data, and using the computer simulation model, we continued our research into the reasons behind the observed trend of ground-level ozone increase in urban and rural areas of Japan. Taking this wider-scale air pollution into consideration, we continued our studies of urban air pollution in Tokyo and Osaka.

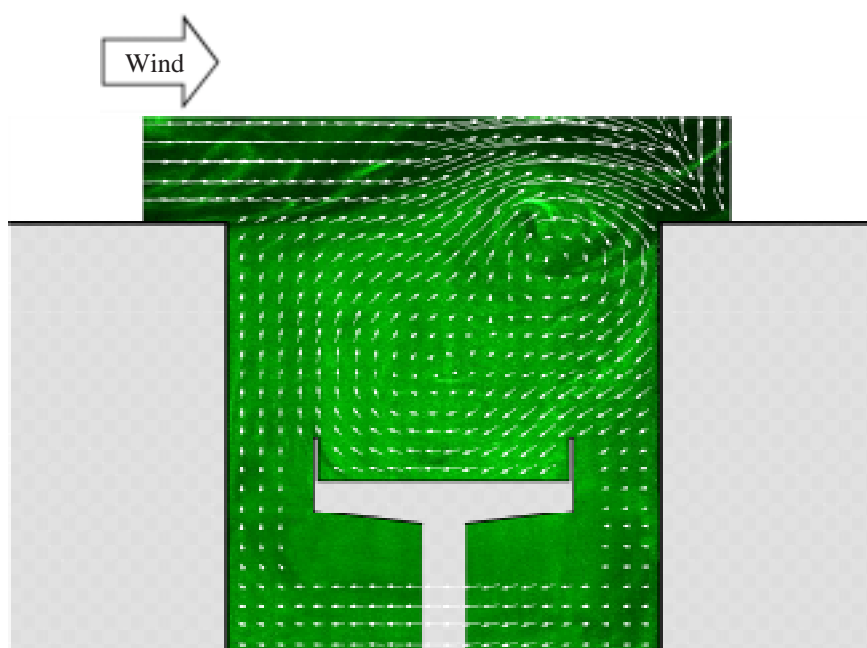


**Fig. 1**  
Wind tunnel experiment:  
An instantaneous vector  
field within the street  
canyon lidded by the  
elevated roadway,  
Measured by Particle  
Image Velocimetry  
(PIV).

### Aerosol Measurement Research Team

The Aerosol Measurement Research Team has been investigating new technologies for measuring particulates and gaseous pollutants. To do this, we have developed a high spatial and temporal resolution monitoring system. We also use a thermal decomposition method to investigate systems for analyzing carbon species. In fiscal year 2002, we conducted a multi-location measurement of NO<sub>2</sub> and particulate matter in a city with heavy traffic. In addition, to examine the applicability of the β-ray absorption method to the measurement of PM<sub>2.5</sub>, we continued our comparison studies with other commonly used methods, such as TEOM and the gravimetric filtration method.

### Epidemiology and Exposure Assessment Research Team

The Epidemiology and Exposure Assessment Research Team is investigating the extent of human exposure to PM<sub>2.5</sub> and DEP. Assessment of exposure is an integral, essential component of environmental epidemiology, risk assessment, and risk management. The methodologies used to assess exposure employ various direct and indirect techniques, such as personal monitoring and modeling. We are currently investigating an exposure modeling approach for airborne PM, based on microenvironmental concentrations and time-activity data. So far, in cooperation with the Traffic Pollution Control Research Team and the Urban Air Quality Research Team, we have conducted a basic study using a GIS to establish an exposure assessment system. We have completed the first-phase model, which can calculate the level of exposure in the population according to the level of pollution concentration, calculated from a diffusion model using concentrations of air pollution emitted from roads and other sources, superimposed on the population distribution. In fiscal year 2002, we proceeded to the second-phase model. The components of the model can include concentrations of PM in typical microenvironments (e.g. homes, roadsides, vehicles) where people spend time; the amount of time spent there; and equations for the relationships between indoor and outdoor concentrations. In metropolitan areas, many people commute a long way to offices or schools, and we therefore need to consider their exposure in these places as well as at home. From the second-phase model, we estimated the DEP exposure of the population of the Kanto region. We also analyzed data on vital statistics in various regions, looking for statistical correlations between exposure levels and mortality rates. We conducted a data analysis on mortality in 13 big cities in Japan to investigate the short-term effects of particulate matter on mortality. These results suggest a positive relationship between PM concentrations and daily mortality in Japan.

### Toxicity and Impact Assessment Research Team

The Toxicity and Impact Assessment Research Team designed toxicological studies to clarify the effects of DEPs – major components of particulate pollutants – and PM<sub>2.5</sub> on respiratory, cardiac and immunological function in rats. Although many articles about the influence of air pollution on human health have been published, few have addressed the effects of diesel exhaust (DE) or DEP on the cardiovascular system. To elucidate the effects of inhalation of DE on cardiac function, we obtained electrocardiograms of young (2 months old) and old (14 months old) rats

exposed to DE at concentrations of 0, 0.3, 1.0, or 3.0 mg DEP/m<sup>3</sup> for 12 h a day, 7 days a week for 6 months. The old rats had a markedly higher frequency of arrhythmias than the young rats at any exposure concentration. The arrhythmias of the young rats were mainly ventricular premature contractions (> 98%), but those of the old rats consisted of atrioventricular block (> 7%) and ventricular premature contraction (< 93%). Our results suggest that inhalation of DE is much more likely to provoke arrhythmias and changes in cardiac function in older rats than in young ones.

We then aimed to determine which chemicals in DEP were affecting cardiovascular function. We attempted to isolate and characterize the compounds in DEP that are responsible for vasodilatation of the rat thoracic artery. We isolated 3 vasodilating nitrophenols, 2-methyl-4-nitrophenol, 3-methyl-4-nitrophenol, and 4-nitrophenol, from a benzene extract of DEP. The concentrations of these nitrophenols were estimated by GC-MS to be 34, 28, and 15 mg/kg DEP, respectively.

We previously showed that DEP enhanced acute lung injury caused by bacterial toxins in mice (Fig. 2(a)-(d)). These effects of DEP were concomitant with the enhanced lung expression of inflammatory molecules such as intercellular adhesion molecule-1, interleukin-1 $\beta$ , macrophage chemoattractant protein-1, keratinocyte chemoattractant, and, in particular, macrophage inflammatory protein-1 $\alpha$ . However, the components of DEP responsible for these effects have not been identified. Currently, we are examining the effects of organic chemicals (DEP-OC) and residual carbonaceous nuclei ('washed DEP') derived from DEP on acute lung injury related to bacterial infection. Both DEP-OC and washed DEP enhanced the infiltration of neutrophils into bronchoalveolar lavage fluid in the presence of bacterial toxin. Washed DEP combined with bacterial toxin synergistically exacerbated pulmonary edema and induced alveolar hemorrhage, which coincided with the enhanced lung expression of interleukin-1 $\beta$ , macrophage inflammatory protein-1 $\alpha$ , macrophage chemoattractant protein-1, and keratinocyte chemoattractant, whereas DEP-OC combined with bacterial toxin did not. The enhancement effects of washed DEP on lipopolysaccharide-related changes were comparable to those of whole DEP. These results suggest that the residual carbonaceous nuclei of DEP, rather than the extracted organic chemicals, are the predominant contributors to the aggravation of lung injury related to bacterial infection. This may be mediated through the expression of proinflammatory molecules, including cytokines and chemokines.

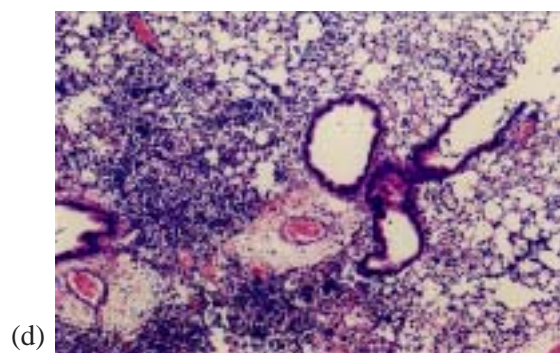
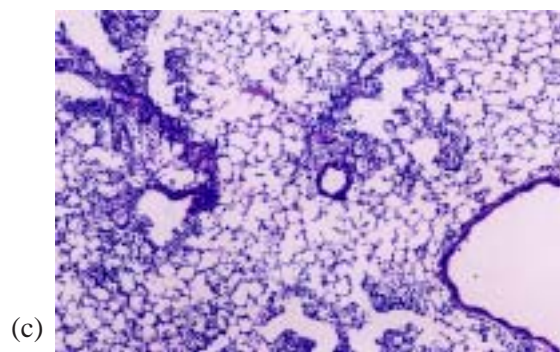
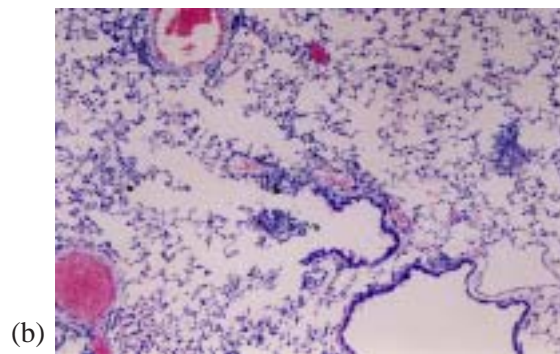
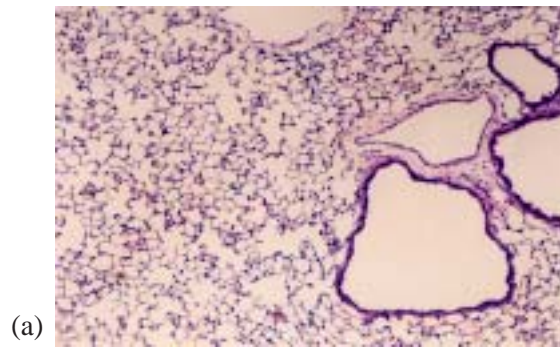


**Fig. 2**

- (a) Lung histology of mice challenged with vehicle exhaust
- (b) Lung histology of mice challenged with DEP
- (c) Lung histology of mice challenged with bacterial toxin
- (d) Lung histology of mice challenged with DEP and bacterial toxin